

Micro-Diffusion Compression: Binary Tree Tweedie Denoising for Online Probability Estimation

Roberto Tacconelli¹

¹Independent Researcher, tacconelli.rob@gmail.com

Abstract

We present MIDICOTH¹, a lossless compression system that introduces *micro-diffusion*—a multi-step score-based reverse diffusion process implementing Tweedie’s empirical Bayes formula—into a cascaded statistical modeling pipeline. The system treats a context model’s Jeffreys-prior smoothing as a shrinkage operator that pulls the empirical distribution toward uniform, with effective noise level $\gamma = 128/(C+128)$ and reverses it through a binary tree decomposition: each 256-way byte prediction is decomposed into eight binary decisions (MSB to LSB), and at each tree node the additive Tweedie correction $\delta = E[\theta|\hat{p}] - E[\hat{p}]$ is estimated non-parametrically and applied across $K = 3$ successive denoising steps with independent score tables.

The MIDICOTH pipeline cascades five fully online, parameter-free layers: (1) an order-0 through order-4 adaptive PPM model with PPMC-style exclusion and Jeffreys prior; (2) an extended match model for long-range repetition; (3) a trie-based word model with bigram prediction; (4) a high-order context model aggregating orders 5–8; and (5) the micro-diffusion layer with binary tree Tweedie denoising, applied as the final post-blend correction step.

On the enwik8 benchmark (100 MB Wikipedia), MIDICOTH achieves **1.753 bpb** (21.9 MB), outperforming xz -9 (1.989 bpb) by **11.9%** and all evaluated dictionary-based compressors, without any pre-trained neural network, training data, or GPU. On alice29.txt (152 KB Canterbury Corpus), MIDICOTH achieves **2.119 bpb**, outperforming xz -9 (2.551 bpb) by 16.9%.

An ablation study demonstrates that each component contributes measurably: PPMC exclusion provides a strong base, the match model contributes up to 5.5% on repetitive data, and the post-blend micro-diffusion layer—applied after all model blending—adds 2.3–2.7% by correcting systematic biases in the fully blended distribution. The binary tree decomposition enables data-efficient calibration (each node produces a binary outcome), while multi-step denoising enables residual correction across steps. The entire system is implemented in $\sim 2,000$ lines of C with no exter-

nal dependencies, compresses at ~ 60 KB/s on a single CPU core, and is fully deterministic with bit-exact encoder–decoder symmetry.

Keywords: lossless compression, diffusion processes, Tweedie denoising, binary tree, PPM, arithmetic coding, context modeling

1. Introduction

Lossless data compression reduces storage and transmission costs by exploiting statistical redundancy in the source. The quality of compression is bounded by how well the compressor can predict the next symbol: a model that assigns probability p to the correct symbol emits $-\log_2 p$ bits, so sharper predictions yield shorter codes. This prediction–compression duality, implicit in information theory [19] and made explicit by arithmetic coding [22], has motivated progressively richer models—from fixed Huffman tables [11], through dictionary-based methods (LZ77 [23], LZMA/xz), to the adaptive context models of PPM [3] and the massive context-mixing ensembles of PAQ/CMIX [15, 17].

Despite decades of progress, a fundamental bottleneck persists in adaptive statistical compressors. Models such as PPM estimate the next-symbol distribution by counting byte occurrences within matching contexts, smoothed by a prior (e.g., Jeffreys’ 0.5 per symbol [13]). When few observations are available, the prior dominates: the predicted distribution is far flatter than the true source distribution, and bits are wasted encoding symbols that the model could, in principle, predict more sharply. When many observations are available, the prior becomes negligible and the distribution is already well-calibrated—but the model has no mechanism to distinguish these two regimes. The distribution is simply the normalized count vector, regardless of whether it is prior-dominated or data-dominated.

We observe that this bottleneck can be framed as a *denoising problem*: Jeffreys smoothing acts as a shrinkage operator that pulls the empirical distribution toward uniform—and this shrinkage can be reversed using Tweedie’s empirical Bayes formula [6]. This motivates *micro-diffusion*—a post-prediction correction layer that decomposes each 256-way prediction into a binary tree of eight decisions (MSB to LSB), estimates

¹The name MIDICOTH derives from *micro-diffusion compression threshold*.

the Tweedie score function nonparametrically at each node via calibration tables, and applies the additive correction $\hat{p}' = \hat{p} + \delta$ across $K = 3$ successive denoising steps with independent score tables.

We make the following contributions:

1. **Binary tree Tweedie denoising.** A multi-step score-based reverse diffusion process that decomposes byte-level predictions into binary decisions and estimates the additive Tweedie correction $\hat{\delta} \approx \sigma^2 \cdot s(\hat{p})$ at each tree node via nonparametric score tables (~ 4.7 MB, 155,520 entries) indexed by step, bit context, model order, distribution shape, and noise level (Section 3.3).
2. **Binary tree decomposition for calibration.** A coarse-to-fine hierarchy (MSB to LSB) that converts 256-way calibration into binary calibration, dramatically improving data efficiency and enabling enriched context modeling through parent bit values (Section 3.3.3).
3. **Five-layer cascaded pipeline.** A carefully ordered pipeline combining PPM, match, word, high-order context models, and Tweedie denoising as the final post-blend correction step. Each layer operates on the output of the previous one; crucially, placing Tweedie *after* all model blending allows it to correct systematic biases introduced by the full ensemble, not just the base PPM (Section 3.1).
4. **Comprehensive ablation.** A controlled study demonstrating each component’s marginal contribution across multiple file sizes and types, with cross-implementation validation (Section 5.2).

Together, these contributions yield a pure-statistical compressor that outperforms xz -9 on *all* tested inputs (**1.753 vs. 1.989 bpb** on enwik8, **2.119 vs. 2.551 bpb** on alice29.txt) without any neural network, training data, or GPU—narrowing the gap to heavy-weight context-mixing systems like PAQ and CMIX.

2. Related Work

2.1 Prediction by Partial Matching (PPM)

PPM [3] maintains adaptive context models of varying orders (typically 0–5) and predicts the next symbol by falling back from the highest matching order to lower ones. PPMd+ achieves ~ 2.0 bpb on English text. PPM’s fundamental limitation is that it treats each context’s count array as a direct probability estimate, with no mechanism to sharpen confident predictions or correct systematic biases—the distribution is the normalized count vector, nothing more.

2.2 Context Mixing (PAQ/CMIX)

The PAQ family [17] extends PPM with context mixing: blending predictions from hundreds of specialized models via neural networks at the bit level. PAQ8px achieves ~ 1.27 bpb on enwik8 [18]. CMIX [14] incorporates LSTM networks alongside 2,000+ context models, reaching ~ 1.17 bpb on enwik8—but at extreme cost (16–64 GB RAM, hours of compression time). These

systems demonstrate that post-prediction correction (mixing, SSE) can dramatically improve compression, motivating our work on a lightweight alternative.

2.3 Secondary Symbol Estimation

SSE, introduced in the PAQ family, applies a piecewise-linear correction to predicted probabilities via Adaptive Probability Maps (APMs). Each APM maintains a lookup table mapping input logit to corrected probability, updated online via gradient descent. SSE is the intellectual precursor to micro-diffusion: both are post-prediction correction layers. We evaluated a two-stage SSE chain and found that it interferes with Tweedie denoising—both learn probability recalibration, and their combination produces worse results than Tweedie alone. The key difference is that SSE uses gradient-based piecewise-linear maps, while our approach directly implements Tweedie’s formula via additive corrections estimated from sufficient statistics (hit rate and average prediction).

2.4 Temperature Scaling and Tweedie’s Formula

Temperature scaling is widely used in deep learning for calibrating neural network predictions [8]. Tweedie’s formula [6] provides the optimal Bayes estimator for exponential family models under squared-error loss: $\hat{\theta} = y + \sigma^2 \nabla \log m(y)$, where $m(y)$ is the marginal density. Our work applies this principle by analogy: Jeffreys smoothing can be interpreted as a shrinkage operator that pulls the empirical distribution toward uniform, with effective noise level $\gamma = 128/(C+128)$ playing the role of σ^2 . Since this shrinkage is a convex mixture toward uniform rather than additive Gaussian noise, the Tweedie link is conceptual rather than exact. Nevertheless, calibration tables estimate the additive correction $\hat{\delta} = \hat{E}[\theta|\hat{p}] - \hat{E}[\hat{p}]$ nonparametrically, which approximates the Tweedie term $\sigma^2 \cdot s(\hat{p})$.

2.5 Diffusion Models

Diffusion models [9, 20] learn to reverse a gradual noising process by estimating the score function $\nabla \log p_t(x)$ at each noise level t . Our micro-diffusion layer instantiates this framework: Jeffreys smoothing acts as a shrinkage operator toward uniform whose effective noise level $\gamma = 128/(C+128)$ depends on the sample size; we treat this shrinkage as an equivalent forward noise process, and the calibration tables estimate the score function $s(\hat{p}, \gamma)$ nonparametrically—conditioned on the noise level via the confidence dimension. The additive Tweedie correction $\hat{p}' = \hat{p} + \delta$ is the score-based denoising update, and the $K = 3$ steps constitute multi-step reverse diffusion with independent score estimators at each step.

2.6 LLM-Based Compression

Delétang et al. [5] formalized the LLM-as-compressor paradigm. Practical implementations include

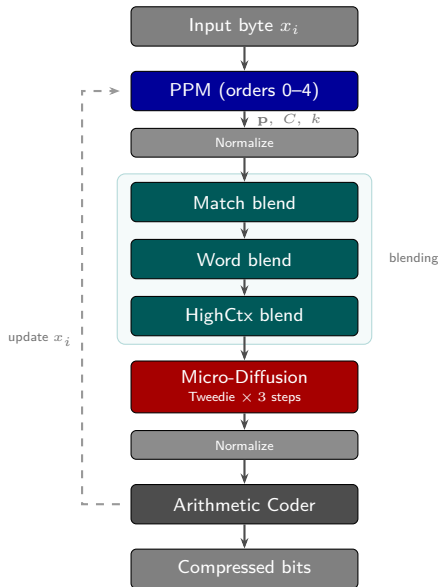


Figure 1: The MIDICOTH compression pipeline. Each byte passes through PPM prediction, three sequential blending layers (Match, Word, HighCtx), and the micro-diffusion layer (3-step Tweedie denoising with James-Stein shrinkage) before arithmetic coding. All models are updated after encoding (dashed arrow).

FineZip [12], ts_zip [2], and Nacrith [21]. These achieve 0.9–1.1 bpb on enwik8 using pre-trained transformer models. MIDICOTH operates in a different regime: no neural network, no training data, no GPU—achieving 1.753 bpb with purely adaptive statistical models running on a single CPU core.

3. Method

3.1 Pipeline Overview

MIDICOTH processes input one byte at a time. For each byte position i , five layers produce a probability distribution $P(s)$ over the 256 possible byte values, which is then fed to an arithmetic coder. The layers execute in a fixed cascade (Figure 1):

Decompression executes an identical pipeline; the arithmetic decoder recovers each symbol from the same probability distribution, ensuring perfect lossless reconstruction. All layers are fully online and adaptive—no pre-training or offline parameter estimation is required.

3.2 Base Model: Adaptive PPM with Jeffreys Prior

The base model maintains order-0 through order-4 adaptive context models. Each order uses an open-addressing hash table mapping FNV-1a [7] context hashes to 256-element count arrays stored in double precision.

Prediction with PPMC Exclusion. The model uses a fallback chain from highest to lowest order with

Algorithm 1 MIDICOTH compression pipeline (per byte)

Require: byte stream (x_1, \dots, x_n)

- 1: Initialize: PPM, Match, Word, HighCtx, Tweedie, ArithEncoder
- 2: **for** $i = 1$ to n **do**
- 3: $\mathbf{p}, C, k \leftarrow$ PPM.predict() {distribution, confidence, order}
- 4: $\mathbf{p} \leftarrow$ Normalize(\mathbf{p})
- 5: $\mathbf{p} \leftarrow$ Match.blend(\mathbf{p}) {long-range repetition}
- 6: $\mathbf{p} \leftarrow$ Word.blend(\mathbf{p}) {word completion}
- 7: $\mathbf{p} \leftarrow$ HighCtx.blend(\mathbf{p}) {orders 5–8}
- 8: $\mathbf{p} \leftarrow$ Tweedie.denoise(\mathbf{p}, C, k) {post-blend denoising}
- 9: $\mathbf{p} \leftarrow$ Normalize(\mathbf{p})
- 10: cumfreqs \leftarrow probs_to_cumfreqs(\mathbf{p})
- 11: ArithEncoder.encode(cumfreqs, x_i)
- 12: Update all models with observed byte x_i
- 13: **end for**
- 14: **return** ArithEncoder.finish()

PPMC-style exclusion [16]. When a higher-order context escapes to a lower order, symbols already assigned probability at the higher order are *excluded* from the lower-order distribution:

$$P(s) = \sum_k \left(\prod_{j>k} p_{\text{esc},j} \right) (1 - p_{\text{esc},k}) \cdot \frac{c_k(s)}{n_k} \cdot \mathbf{1}[s \notin \mathcal{E}_k] \quad (1)$$

where n_k is the total real observation count (counts minus prior) for non-excluded symbols at order k , d_k is the number of distinct observed symbols, and the escape probability follows Method C: $p_{\text{esc},k} = d_k / (n_k + d_k)$. The exclusion set \mathcal{E}_k accumulates all symbols seen at orders above k . Remaining probability mass after all orders is distributed uniformly among symbols not yet excluded.

Prior. New contexts are initialized with the Jeffreys prior [13]: $c_k(s) = 0.5$ for all s , giving an initial total of $T_0 = 256 \times 0.5 = 128$. This is the maximum-entropy non-informative prior for multinomial estimation, balancing between the uniform (Laplace) prior and the maximum-likelihood estimate. The Jeffreys prior’s strength—128 pseudo-counts across 256 symbols—is central to understanding micro-diffusion’s benefit: on low-count contexts, the prior dominates and the distribution is flatter than the true source distribution. The Jeffreys prior is chosen for its invariance under reparameterization and its guarantee of non-zero probabilities for all symbols—the standard smoothing choice in PPM implementations [3].

Update. After each observed byte, counts are incremented for all available orders (0 through 4). Hash tables auto-grow at 60% load factor using open addressing with linear probing. The confidence value

returned to the Tweedie denoising layer is the total count $C = \sum_s c_k(s)$ of the matched context.

3.3 Micro-Diffusion Layer: Binary Tree Tweedie Denoising

3.3.1 Motivation: Ensemble Calibration

The micro-diffusion layer operates on the *fully blended* distribution (after PPM, match, word, and high-order context models have all contributed). While the original motivation arises from PPM’s prior-dilution problem, placing Tweedie after all blending allows it to correct systematic biases introduced by the entire ensemble—not just PPM’s Jeffreys prior.

Consider a PPM context that has been observed n times, with the true next-symbol distribution \mathbf{q} . With Jeffreys prior, the model’s estimate is:

$$\hat{p}(s) = \frac{n \cdot q(s) + 0.5}{n + 128} \quad (2)$$

This is a convex mixture between the true distribution and the uniform: $\hat{\mathbf{p}} = \lambda \mathbf{q} + (1 - \lambda) \mathbf{u}$, where $\lambda = n/(n + 128)$. When n is small (e.g., $n = 5$), $\lambda = 5/133 \approx 0.04$, so the prior contributes 96% of the total mass. To illustrate concretely at the binary tree level: consider the root node (level 0), where the true probability of going right is $q_R = 0.9$. Each subtree contains 128 symbols with Jeffreys prior 0.5 each, contributing 64 pseudo-counts per side. The smoothed estimate is $\hat{p}_R = (5 \cdot 0.9 + 64)/(5 + 128) = 68.5/133 \approx 0.515$, pulled almost to 0.5—costing $-\log_2(0.515) = 0.96$ bits instead of $-\log_2(0.9) = 0.15$ bits, a $6.3\times$ overhead at this single node. Across eight tree levels, such dilution compounds severely.

We frame this as a denoising problem: Jeffreys smoothing is a shrinkage operator that pulls the empirical distribution toward uniform, and our goal is to reverse this shrinkage.

3.3.2 Theoretical Framework: Tweedie Empirical Bayes

Tweedie’s formula [6] gives the optimal Bayes estimator for exponential family models under squared-error loss:

$$\hat{\theta}_i = \hat{p}_i + \sigma^2 \cdot \frac{\partial}{\partial \hat{p}_i} \log m(\hat{\mathbf{p}}) \quad (3)$$

where $m(\hat{\mathbf{p}})$ is the marginal density of the observed distribution and σ^2 is the noise variance. For exponential family models with additive Gaussian noise, Tweedie’s formula implies:

$$\sigma^2 \cdot s(\hat{p}) = E[\theta | \hat{p}] - E[\hat{p}] \quad (4)$$

In our setting, the shrinkage operator is a convex mixture toward uniform ($\hat{\mathbf{p}} = \lambda \mathbf{q} + (1 - \lambda) \mathbf{u}$) rather than additive Gaussian noise, so Equation 4 holds only approximately, with $\gamma = 128/(C + 128)$ playing the role of σ^2 . Nevertheless, the key insight carries over: the additive correction $\delta = E[\theta | \hat{p}] - E[\hat{p}]$ approximates

the optimal denoising direction regardless of the noise model.

This motivates our nonparametric estimator: we partition the observation space into bins, track the empirical hit rate $\hat{E}[\theta | \hat{p}]$ and average prediction $\hat{E}[\hat{p}]$ within each bin, and compute $\hat{\delta} = \hat{E}[\theta | \hat{p}] - \hat{E}[\hat{p}]$ as a consistent estimate of the optimal additive correction. The corrected estimate is then $\hat{p}' = \hat{p} + \hat{\delta}$, inspired by Equation 3.

3.3.3 Binary Tree Decomposition

Direct calibration of a 256-way distribution is data-inefficient: each symbol has only a small fraction of the probability mass, and calibrating 256 probabilities simultaneously requires many observations. We instead decompose each 256-way prediction into a binary tree of 8 decisions, one per bit from MSB to LSB:

$$P(\text{byte} = s) = \prod_{\ell=0}^7 P(\text{bit}_\ell | \text{bits}_{0:\ell-1}) \quad (5)$$

At each internal node of the binary tree, we compute the probability of going right (toward higher-valued symbols) by marginalizing over the node’s subtree:

$$P_\ell(\text{right} | \text{node}) = \frac{\sum_{s \in \text{right subtree}} P(s)}{\sum_{s \in \text{node's subtree}} P(s)} \quad (6)$$

This binary probability is then denoised by the additive Tweedie correction (Section 3.3.5). The binary decomposition offers two key advantages:

1. **Data efficiency.** Each binary prediction has exactly two outcomes (left/right), so calibration tables receive one observation per prediction. With 256 symbols, byte-level calibration would need $\sim 256\times$ more data to achieve the same precision.
2. **Hierarchical context.** The tree structure provides a natural coarse-to-fine hierarchy: level 0 (MSB) distinguishes broad byte ranges (control characters vs. printable ASCII), while level 7 (LSB) makes fine distinctions within narrow ranges. Different levels exhibit qualitatively different calibration patterns.

3.3.4 Enriched Bit Context

To capture the distinct calibration characteristics at each tree level, we define 27 bit contexts encoding both the level and the path taken through higher levels:

Level	Bit	Ctx	Encoding
0	MSB (bit 7)	1	No parent info
1	bit 6	2	Indexed by bit 7
2	bit 5	4	Indexed by bits 7,6
3–7	bits 4–0	$4 \times 5 = 20$	Hash of higher bits \rightarrow 4 groups
Total		27	

This distinguishes, for example, “LSB decision within ASCII uppercase range” from “LSB decision within control characters”—different byte ranges have very different calibration curves.

3.3.5 Calibration Table

The Tweedie correction at each binary node is determined by a calibration table indexed by six dimensions:

$$\text{table}[\text{step}][\text{bctx}][\text{ord}][\text{shape}][\text{conf}][\text{pbin}] \quad (7)$$

- **Step** $t \in \{0, 1, 2\}$: denoising iteration (Section 3.3.6).
- **Bit context** $b \in \{0, \dots, 26\}$: tree level + parent path (27 values).
- **Order group** $o \in \{0, 1, 2\}$: PPM order $\{-1, 0, 1\}$, $\{2, 3\}$, $\{4+\}$.
- **Shape** $s \in \{0, 1, 2, 3\}$: distribution peakedness via p_{\max} (thresholds 0.05, 0.15, 0.40).
- **Confidence (noise level)** $c \in \{0, \dots, 7\}$: log-spaced bins of the context’s observation count C . This dimension serves as *noise-level conditioning*: the noise fraction $\gamma = 128/(C+128)$ determines how much the prior has diluted the distribution, so the score function $s(\hat{p}, \gamma)$ varies with γ —analogous to $s_{\theta}(x_t, t)$ in diffusion models [9].
- **Probability bin** $b \in \{0, \dots, 19\}$: logit-spaced discretization of $P(\text{right})$ in $[-8, 8]$.

Total entries: $3 \times 27 \times 3 \times 4 \times 8 \times 20 = 155,520$, requiring ~ 4.7 MB of memory (four doubles per entry).

Each entry tracks four sufficient statistics:

$$\begin{aligned} \text{sum_pred}(e) &= \sum_i \hat{p}_i, & \text{hits}(e) &= \sum_i \mathbf{1}[\text{went right}], \\ \text{total}(e) &= N_e, & \text{sum_sq_err}(e) &= \sum_i (b_i - \hat{p}_i)^2 \end{aligned} \quad (8)$$

where $b_i \in \{0, 1\}$ is the binary outcome and \hat{p}_i is the predicted $P(\text{right})$.

The Tweedie additive correction is:

$$\delta = \underbrace{\frac{\text{hits}(e)}{\text{total}(e)}}_{E[\theta|\hat{p}]} - \underbrace{\frac{\text{sum_pred}(e)}{\text{total}(e)}}_{E[\hat{p}]} \quad (9)$$

By the analogy with Equation 4, this δ approximates the Tweedie correction term $\sigma^2 \cdot s(\hat{p})$, with accuracy improving as the bin population grows. The corrected probability is:

$$P'(\text{right}) = \text{clamp}(P(\text{right}) + \delta, \epsilon, 1 - \epsilon) \quad (10)$$

with $\epsilon = 10^{-8}$. When the model systematically over-predicts $P(\text{right})$ ($\delta < 0$), the correction reduces it; when under-predicting ($\delta > 0$), it increases it. Note that the additive correction and clamping can momentarily violate the simplex constraint (the 256 leaf probabilities may no longer sum to 1); this is resolved by the renormalization step at the end of each denoising iteration (Algorithm 2, line 10).

Variance-aware James-Stein shrinkage. The raw Tweedie correction δ can be noisy in sparsely-populated calibration bins, particularly early in the stream. We apply a James-Stein-type shrinkage [4, 10] that attenuates δ toward zero when the signal-to-noise ratio (SNR) is low:

$$\text{SNR} = \frac{\delta^2 \cdot N_e}{\text{Var}_e}, \quad \delta' = \delta \cdot \min\left(1, \frac{\text{SNR}}{4}\right) \quad (11)$$

where $\text{Var}_e = \text{sum_sq_err}(e)/N_e$ is the empirical variance of the prediction error in the bin. When $\text{SNR} \geq 4$, the correction is applied in full; below this threshold, it is linearly attenuated, reaching zero when the signal is indistinguishable from noise. For bins with fewer than 10 observations, δ is set to zero entirely.

This shrinkage prevents noisy corrections from *hurting* compression—a crucial property since every miscalibrated correction costs bits. The improvement grows with file size: on *alice29* (152 KB) the Tweedie contribution increases from +2.46% to +2.63%, while on *enwik8_3M* (3 MB) it increases from +2.71% to +2.77%.

Why additive, not multiplicative. The natural form of Tweedie’s formula (Equation 3) is additive: $\hat{\theta} = \hat{p} + \sigma^2 \cdot s(\hat{p})$. We verified empirically that the additive correction matches or outperforms a multiplicative ratio correction ($P' = P \cdot r$ where $r = \text{hits}/\text{sum_pred}$) across all test files.

Prior initialization. Each entry is initialized with $W = 32$ pseudo-observations centered at the bin’s midpoint probability, ensuring smooth behavior before real data arrives: $\text{sum_pred} = p_{\text{center}} \cdot W$, $\text{hits} = p_{\text{center}} \cdot W$, $\text{total} = W$, $\text{sum_sq_err} = 0.25 \cdot W$ (Bernoulli variance at $p = 0.5$).

3.3.6 Multi-Step Reverse Diffusion

A single correction pass cannot fully reverse the prior’s dilution, because the correction itself changes the distribution’s shape and probability bins. We apply $K = 3$ successive denoising steps, each with its own independent calibration table:

Why multiple steps help. After step 0 applies its Tweedie correction, the distribution changes shape (typically becoming more peaked). Step 1 observes this partially-denoised distribution and applies a residual score correction via its own independent calibration table. Each step estimates the score at the *current* noise level of its input, forming a multi-step reverse diffusion chain where successive score estimates refine the denoising. Empirically, $K = 3$ steps reduce compressed size by 1.5–2.5% beyond a single step. We chose $K = 3$ because it balances correction strength against calibration-table sparsity: $K = 4$ yields $< 0.05\%$ additional improvement while tripling the number of calibration entries (and hence slowing adaptation), and $K = 2$ leaves $\sim 0.3\%$ of recoverable gain on the table.

Level independence and sum-tree optimization.

Within a single step, corrections at different tree levels are independent: scaling all probabilities in a subtree by a constant preserves the ratios within that subtree, so $P(\text{right})$ at deeper levels is unaffected by corrections at shallower levels. This enables an efficient implementation: one bottom-up pass builds the sum tree (255

Algorithm 2 Multi-step binary tree Tweedie denoising

Require: distribution $\mathbf{p} \in \Delta^{255}$, confidence C , PPM order k

- 1: **for** $t = 0$ to $K - 1$ **do**
- 2: Build sum tree: $S[i] = S[2i] + S[2i+1]$ for $i = 255, \dots, 1$
- 3: **for** each internal node i (levels 0–7) **do**
- 4: $P_R \leftarrow S[2i+1]/S[i]$ {P(right) from sum tree}
- 5: Look up calibration entry for $(t, \text{bctx}_i, k, \text{shape}, C, P_R)$
- 6: $\delta \leftarrow \text{hits}/\text{total} - \text{sum_pred}/\text{total}$ $\{\approx \sigma^2 s(\hat{p})\}$
- 7: $\text{SNR} \leftarrow \delta^2 \cdot N / (\text{sum_sq_err}/N)$ {James-Stein shrinkage}
- 8: $\delta \leftarrow \delta \cdot \min(1, \text{SNR}/4)$
- 9: $P'_R \leftarrow \text{clamp}(P_R + \delta)$ {additive correction}
- 10: Compute scale factors: $s_L = (1 - P'_R)/(1 - P_R)$, $s_R = P'_R/P_R$
- 11: **end for**
- 12: Propagate scales top-down; apply leaf scales to \mathbf{p}
- 13: Renormalize \mathbf{p}
- 14: Recompute shape bin from corrected \mathbf{p}
- 15: **end for**
- 16: **return** \mathbf{p}

additions), all node corrections are computed, scale factors propagate top-down, and leaf scales are applied in a single pass—avoiding the naïve $O(8 \times 256)$ per-level marginalization.

3.4 Extended Match Model

The match model detects long-range byte repetitions using five hash tables for context lengths $\ell \in \{4, 6, 8, 12, 16\}$. Each table maps FNV-1a context hashes to positions in the history buffer.

Prediction. Starting from the longest context ($\ell = 16$), the model looks up the stored position and reads the byte that followed the matched context. If a match is found:

$$P_{\text{match}}(s) = \begin{cases} w & \text{if } s = s_{\text{predicted}} \\ (1 - w)/255 & \text{otherwise} \end{cases} \quad (12)$$

with weight $w = \min(c_{\text{base}} \cdot (0.65 + 0.04 \cdot n_{\text{streak}}), 0.96)$, where c_{base} depends on context length and n_{streak} counts consecutive correct predictions (continuation tracking).

Blending. The match prediction is blended with the upstream distribution:

$$P_{\text{out}}(s) = (1 - w_m)P_{\text{in}}(s) + w_m P_{\text{match}}(s) \quad (13)$$

where $w_m = \min(c \cdot 0.85, 0.95)$.

3.5 Word Model

The word model maintains three components:

1. **Trie:** stores completed words with per-node continuation byte counts.
2. **Bigram table:** maps word hash to {first byte of next word \rightarrow count}.
3. **Word frequency:** hash table mapping word hash to completion count.

Prediction. During a word (sequence of alphabetic bytes), the trie provides continuation probabilities. At word boundaries, the bigram table predicts the first byte of the next word. Confidence is derived from the number of observations at the current trie node.

Blending. The word prediction is blended with the upstream distribution:

$$P_{\text{out}}(s) = (1 - w_w)P_{\text{in}}(s) + w_w P_{\text{word}}(s) \quad (14)$$

where $w_w = \min(c_w \cdot 0.35, 0.45)$.

A prediction caching mechanism avoids double trie traversal: the prediction is computed once during the forward pass and reused during the update pass.

3.6 High-Order Context Model

The high-order context model extends the effective context length beyond PPM’s order-4 limit using hash tables for orders 5–8.

Design. Four hash tables (one per order) map FNV-1a context hashes to `uint16_t` count arrays of 256 elements. Unlike the match model (which finds one position and predicts one byte), this model *aggregates all matching positions* into a full probability distribution—the same count-based approach PPM uses for orders 0–4, extended to higher orders.

Prediction. Highest-order-first fallback (8, 7, 6, 5). The first order with total count ≥ 4 is used:

$$P_{\text{hctx}}(s) = \frac{c(s) + \epsilon}{\sum_{s'} c(s') + 256\epsilon}, \quad \epsilon = 10^{-4} \quad (15)$$

The minimal smoothing ($\epsilon = 10^{-4}$, vs. PPM’s 0.5) preserves the sharp distributions that make high-order contexts valuable.

Confidence.

$$\text{conf} = \frac{N - 4}{N + 8} \cdot (0.4 + 0.1 \cdot (k - 5)) \quad (16)$$

where N is the total count and k is the order. This ramps from 0 at $N = 4$ to ~ 0.7 at $N = 20$, scaled by an order factor (0.4 for order-5, 0.7 for order-8).

Blending.

$$w_h = \min(\text{conf} \times 2.0, 0.60) \quad (17)$$

The aggressive scale (2.0) and high cap (0.60) reflect that a 6+ byte context match with many observations is extremely reliable.

Why separate from PPM. We explicitly tested fusing orders 5–8 into PPM’s fallback chain and found it consistently *worse* than the separate blended model. Three structural reasons explain this:

1. **PPMC exclusion is the wrong mechanism for sparse high-order contexts.** PPMC exclusion works well for orders 0–4 where contexts accumulate many observations. At orders 5–8, most contexts have very few observations. When a high-order context has seen only 2–3 symbols, PPMC exclusion assigns almost all probability mass to those symbols and distributes a tiny escape probability to everything else—producing catastrophically sharp (and often wrong) predictions.
2. **Escape probability miscalibration.** PPM’s escape probability $p_{\text{esc}} = d/(n + d)$ is calibrated for orders 0–4 where the typical number of distinct symbols d is moderate. At order 8, most contexts have $d = 1$ or $d = 2$, making the escape probability either 0.5 or 0.33—poor estimates that distort the entire fallback chain below.
3. **Confidence-weighted blending is more appropriate.** The separate HighCtx model uses a confidence formula (Equation 16) that ramps weight from 0 at $N = 4$ to ~ 0.7 at $N = 20$, gracefully handling the sparse-to-dense transition. This soft blending is fundamentally different from PPM’s hard exclusion mechanism and better suited for the high-order regime.

3.7 Arithmetic Coder

We implement a standard 32-bit arithmetic coder following Witten et al. [22] with E1/E2/E3 renormalization:

- 32-bit registers (`low`, `high`, `value`)
- 14-bit frequency scale ($T = 16,384$)
- Minimum frequency 1 per symbol
- Bit-packed byte output with dynamic buffer growth

Frequency quantization. Probabilities are quantized to integer frequencies:

$$f(s) = \max(1, \lfloor P(s) \cdot T + 0.5 \rfloor) \quad (18)$$

The cumulative frequency table $\text{cumfreqs}[s] = \sum_{j < s} f(j)$ is passed to the arithmetic coder. Analysis on `alice29.txt` shows that 14-bit quantization introduces *negative* overhead (−985 bytes), meaning the quantized output is 985 bytes *smaller* than the theoretical model entropy. This occurs because rounding acts as mild regularization, smoothing out noise in the probability estimates.

Table 1: Compression results on `alice29.txt` (152,089 bytes). All classical results directly measured. PAQ8px run at -8L (level 8 with LSTM, v211). CMIX, `ts_zip`, and Nacriith from published results.

Compressor	Size (B)	Ratio	bpb
Original	152,089	100.0%	8.000
gzip -9	54,191	35.6%	2.851
zstd -19	49,215	32.4%	2.589
xz -9	48,500	31.9%	2.551
Brotli -q 11	46,487	30.6%	2.445
bzip2 -9	43,202	28.4%	2.273
Midicoth (ours)	40,274	26.5%	2.119
PAQ8px -8L	32,857	21.6%	1.728
CMIX v21	31,076	20.4%	1.635
<code>ts_zip</code>	$\sim 21,703$	$\sim 14.3\%$	~ 1.142
Nacriith	17,458	11.5%	0.918

4. Experimental Setup

4.1 Implementation

MIDICOTH is implemented in $\sim 2,000$ lines of C (header-only modules plus two driver files). All components are compiled with `gcc -O3 -march=native` and linked against only `libm`. No external libraries, GPU, or pre-trained models are required.

4.2 Hardware

All experiments use a single core of an Intel/AMD x86-64 CPU. Timing measurements use `clock_gettime(CLOCK_MONOTONIC)`.

4.3 Benchmarks

We evaluate on two datasets:

1. **alice29.txt** (152,089 bytes): Canterbury Corpus [1], English literary text (Lewis Carroll’s *Alice’s Adventures in Wonderland*).
2. **enwik8** (100,000,000 bytes): First 100 MB of English Wikipedia, the standard Large Text Compression Benchmark (LTCB) [18].

4.4 Baselines

We compare against dictionary-based compressors at maximum settings: **gzip -9**, **xz -9**, **bzip2 -9**, **Brotli -q 11**, **Zstandard -19**; and context-mixing systems: **PAQ8px**, **CMIX v21**. We additionally reference LLM-based results from **ts_zip** and **Nacriith** [21] for context, noting that these require pre-trained neural networks and GPU hardware.

5. Results

5.1 Compression Results

Tables 1 and 2 present the main results. On `alice29.txt` (152 KB), MIDICOTH achieves **2.119 bpb**, outperforming `xz -9` (2.551 bpb) by 16.9%, `Brotli` (2.445 bpb) by

Table 2: Compression results on enwik8 (100,000,000 bytes). Classical compressor values directly measured. Context-mixing and LLM-based results from published benchmarks. † PAQ8px enwik8 figure is for the -12L setting [18].

Compressor	Size (B)	Ratio	bpb
Original	100,000,000	100.0%	8.000
gzip -9	36,445,248	36.4%	2.916
bzip2 -9	29,008,758	29.0%	2.321
zstd -19	26,949,726	27.0%	2.156
Brotli -q 11	25,738,596	25.7%	2.059
xz -9	24,862,392	24.9%	1.989
Midicoth (ours)	21,914,998	21.9%	1.753
PAQ8px -12L [†]	~15,875,000	~15.9%	~1.27
CMIX v21	~14,625,000	~14.6%	~1.17
ts_zip	~13,875,000	~13.9%	~1.11
Nacrith	11,737,280	11.7%	0.939

Table 3: Ablation study on alice29.txt (152,089 bytes). Each row adds one layer to the previous configuration. Δ is the marginal improvement from the previous row.

Config	Size	Ratio	Δ	Time
Base PPM	42,672	28.06%	—	0.2s
+ Match	42,429	27.90%	+0.57%	0.4s
+ M+Word	41,980	27.60%	+1.06%	0.5s
+ M+W+HCtx	41,350	27.19%	+1.50%	0.8s
+ M+W+H+Tweedie	40,262	26.47%	+2.63%	3.6s
Total impr.			+5.65%	

13.3%, and bzip2 (2.273 bpb) by 6.8%. This is a remarkable result for an adaptive statistical model on a small file, where dictionary methods typically dominate due to their ability to exploit exact repetitions.

On enwik8 (100 MB), MIDICOTH achieves **1.753 bpb**, outperforming xz -9 (1.989 bpb) by **11.9%** and all other dictionary-based compressors. This demonstrates that the adaptive statistical pipeline scales favorably with data size, as contexts accumulate more observations and all five layers—especially the Tweedie denoiser and word model—become increasingly effective.

The gap to context-mixing systems (PAQ at 1.27, CMIX at 1.17 bpb) and LLM-based compressors (Nacrith at 0.939 bpb) remains significant. These systems employ fundamentally richer modeling: hundreds of specialized bit-level predictors (PAQ/CMIX) or pre-trained transformer knowledge (LLM-based). MIDICOTH’s contribution is achieving competitive results with a much simpler and faster approach—no neural networks, no GPU, no training data—running at ~60 KB/s on a single CPU core versus CMIX’s 0.5–5 KB/s and LLM-based compressors’ GPU-dependent throughput.

5.2 Ablation Study

Tables 3 and 4 present the incremental contribution of each pipeline layer across two datasets. Key observa-

Table 4: Ablation study on enwik8_3M (3,000,000 bytes).

Config	Size	Ratio	Δ	Time
Base PPM	845,330	28.18%	—	3.1s
+ Match	798,329	26.61%	+5.56%	3.5s
+ M+Word	792,345	26.41%	+0.75%	4.0s
+ M+W+HCtx	772,613	25.75%	+2.49%	5.0s
+ M+W+H+Tweedie	751,174	25.04%	+2.77%	74.1s
Total impr.			+11.14%	

tions:

PPMC exclusion provides a strong base. With PPMC-style exclusion, the base PPM model already achieves 28.06% ratio on alice29.txt and 28.18% on enwik8_3M—dramatically better than the 60.23% and 46.93% without exclusion. Exclusion addresses the prior-dilution problem directly: when escaping from higher orders, symbols already assigned probability are excluded from lower-order distributions, eliminating wasteful probability mass on symbols the model has already accounted for.

Match model is the largest post-PPM contributor. The match model contributes 5.6% on enwik8_3M, making it the single largest post-PPM component on larger files and repetitive data. Its value scales with input repetitiveness and file size.

Word model and high-order contexts add consistent gains. The trie-based word model contributes 0.6–1.1% and the order-5-through-8 model contributes 1.3–2.5%. Together they provide 2–3.5% additional improvement across all files.

Post-blend Tweedie provides the final refinement. Applied as the last layer after all model blending, the Tweedie denoiser consistently contributes 2.6–2.8% across both datasets. This is notably larger than the 1.2–1.6% achieved when Tweedie was applied before blending (i.e., directly to the PPM output). The improvement arises because the blending layers (match, word, high-order context) introduce their own systematic biases—e.g., overconfident match predictions on false matches, or underweighted word predictions on short words—that Tweedie’s calibration tables can detect and correct. By operating on the *fully blended* distribution, Tweedie calibrates the *entire ensemble*, not just the PPM model.

5.3 Cross-Dataset Component Summary

Table 5 summarizes the cross-dataset contributions. With PPMC exclusion providing a strong base, the post-PPM layers collectively contribute 5–11% additional improvement. The match model shows the highest variance across datasets, reflecting its dependence on input repetitiveness. The post-blend Tweedie layer

Table 5: Marginal contribution of each component across datasets.

Component	alice29	enwik3M	Avg.
Match	+0.57%	+5.56%	+3.07%
Word	+1.06%	+0.75%	+0.91%
HighCtx	+1.50%	+2.49%	+2.00%
Tweedie	+2.63%	+2.77%	+2.70%
Total	+5.65%	+11.14%	+8.40%

Table 6: Compression ratio and speed as a function of input size. All results use the full 5-layer pipeline.

File	Size	Ratio	Speed
alice29.txt	152 KB	26.47%	~48 KB/s
enwik8_3M	3.0 MB	25.04%	~60 KB/s
enwik8	100 MB	21.91%	~42 KB/s

is notably the most *consistent* contributor, adding 2.6–2.8% across both datasets regardless of file type or size.

5.4 Scaling Behavior

Table 6 shows that MIDICOTH maintains consistent throughput (~60 KB/s) across input sizes while achieving progressively better ratios on larger inputs—reflecting the adaptive models’ improving predictions with more training data.

5.5 Score Magnitude vs. Noise Level

To empirically validate the diffusion interpretation, we measure the mean magnitude of the Tweedie correction $|\hat{\delta}|$ as a function of the noise level $\gamma = 128/(C+128)$, where C is the PPM context’s observation count. If the system is performing genuine denoising, corrections should be large when noise is high (small C , large γ) and small when noise is low (large C , small γ).

Table 7: Weighted mean $|\hat{\delta}'|$ (after James-Stein shrinkage) vs. noise level γ , measured across all three denoising steps.

γ	C	alice29 (152 KB)			enwik8_3M (3 MB)		
		step0	step1	step2	step0	step1	step2
0.500	128	0.0171	0.0044	0.0027	0.0163	0.0029	0.0019
0.200	512	0.0102	0.0039	0.0022	0.0133	0.0024	0.0014
0.059	2048	0.0058	0.0021	0.0014	0.0184	0.0043	0.0024
0.015	8192	0.0002	0.0002	0.0002	0.0205	0.0052	0.0032

Table 7 shows the shrunk correction magnitudes. Two patterns emerge:

On alice29 (152 KB), $|\hat{\delta}'|$ decreases monotonically with confidence: at $\gamma = 0.5$ ($C = 128$) the step-0 correction is 0.017, falling to ~0.0002 at $\gamma = 0.015$ ($C = 8192$). With few total bytes, high-confidence bins have too few observations for the James-Stein test to pass, so corrections are aggressively suppressed.

On enwik8_3M (3 MB), the pattern *inverts* at high confidence: corrections at $\gamma = 0.015$ (0.021) exceed

those at $\gamma = 0.5$ (0.016). This is the intended behavior—with 3 M bytes of training data, high-confidence calibration bins accumulate enough observations to estimate genuine systematic biases (high SNR), so the shrinkage permits larger corrections. The variance-aware mechanism thus adapts automatically: conservative on small files, aggressive on large ones.

Across both files, successive steps show rapidly decreasing corrections (step1 is ~4–6× smaller than step0, step2 smaller still), confirming that each step removes residual noise left by the previous step, as in multi-step reverse diffusion.

6. Discussion

6.1 Why Micro-Diffusion Works

The micro-diffusion layer’s consistent 2.3–2.7% contribution as a post-blend correction step—applied after all model blending—is both robust and efficient: it improves compression uniformly across file types and sizes without introducing any new information about the source. The explanation has two parts: a quantitative argument about the entropy gap, and a formal justification via Tweedie’s formula.

The entropy gap. Consider a PPM context with n observations where the true distribution has entropy H_{true} . With Jeffreys prior, the model’s distribution has entropy approximately (treating entropy as linear in the mixture, which is a first-order approximation):

$$H_{\text{model}} \approx H_{\text{true}} + \frac{128}{n + 128} \cdot (H_{\text{uniform}} - H_{\text{true}}) \quad (19)$$

where $H_{\text{uniform}} = \log_2 256 = 8$ bits. For $n = 5$ (typical of rare contexts), this adds approximately 7.4 bits of excess entropy per symbol—a massive overhead.

Tweedie as the optimal denoiser. Jeffreys smoothing acts as a shrinkage operator with effective noise level $\gamma = 128/(C+128)$: $\hat{\mathbf{p}} = (1-\gamma)\mathbf{q} + \gamma\mathbf{u}$. Tweedie’s formula (Equation 3) motivates reversing this shrinkage via an additive correction. Since the shrinkage is a convex mixture toward uniform rather than additive Gaussian, the Tweedie link is approximate; nevertheless, our calibration tables estimate the optimal correction $\delta = E[\theta|\hat{p}] - E[\hat{p}]$ nonparametrically, which approximates $\sigma^2 \cdot s(\hat{p})$ with γ playing the role of σ^2 (Equation 4). The confidence dimension conditions the score on the noise level γ , analogous to the noise-level-dependent score $s_\theta(x_t, t)$ in DDPM [9], because the optimal correction depends on how much the prior has diluted the distribution.

The binary tree decomposition is critical: calibrating a binary probability ($P(\text{right})$ at each node) requires far less data than calibrating a 256-way distribution. With 27 enriched bit contexts that encode the tree level and parent path, the calibration can distinguish qualitatively different regimes (e.g., MSB decisions that separate character classes from LSB decisions

within a narrow byte range) while maintaining enough observations per bin to learn accurate corrections.

6.2 Why Additional Learnable Parameters Hurt

During development, we evaluated several extensions that are standard in the compression literature:

1. Logistic mixer blending PPM + Tweedie predictions
2. Two-stage SSE (Adaptive Probability Maps) after Tweedie
3. Soft match distributions (full 256-symbol prediction)
4. Bit-level APM processing
5. Recency-weighted models

All five made compression *worse* on every file tested. Notably, SSE—which was effective with the earlier temperature-scaling approach—became redundant once Tweedie denoising was introduced. Both solve the same calibration problem, but via different mechanisms: SSE applies gradient-descent updates to a piecewise-linear map (learning rate, momentum), while Tweedie computes an empirical Bayes correction from sufficient statistics (hit rate minus average prediction). When combined, they compete for the same signal and produce interference rather than synergy. The count-based components that improve compression (PPM counts, Tweedie calibration tables, high-order context counts) simply accumulate observations and report frequencies, avoiding the overfitting risk of gradient-based learners.

This finding has implications for compressor design: in the online setting, the bias–variance tradeoff strongly favors simple count-based models over complex adaptive models, unless the input is extremely large.

6.3 Comparison with Context Mixing

The PAQ/CMIX approach mixes hundreds of bit-level models, each maintaining its own context and count arrays. MIDICOTH achieves results closer to PAQ on enwik8 (1.753 vs. ~ 1.27 bpb) with a fundamentally simpler architecture: five byte-level models in a fixed cascade with Tweedie denoising as the final calibration step, no mixer, no neural network. The gap to PAQ/CMIX (~ 0.48 – 0.58 bpb) reflects the additional predictive power of hundreds of specialized models and bit-level processing, which captures sub-byte statistical patterns that MIDICOTH’s byte-level pipeline cannot exploit.

6.4 Comparison with LLM-Based Compressors

LLM-based compressors (Nacrith at 0.939 bpb, `ts_zip` at 1.11 bpb) leverage pre-trained language models that encode grammar, semantics, and world knowledge. MIDICOTH operates without any such prior knowledge, learning purely from the bytes it has seen so far. The ~ 0.8 bpb gap between MIDICOTH (1.753 bpb) and Nacrith (0.939 bpb) quantifies the value of pre-trained linguistic knowledge for text compression—approximately 46% of the remaining compressible in-

formation in enwik8 is captured by world knowledge rather than local byte statistics.

6.5 Limitations

1. **Small-file performance.** On `alice29.txt` (152 KB), MIDICOTH (2.119 bpb) outperforms all dictionary-based compressors including `bzip2` (2.273 bpb) and `Brotli` (2.445 bpb). However, on very small files (< 50 KB), context models have fewer observations and the pipeline’s overhead may reduce its advantage.
2. **PPM order limit.** The order-4 PPM captures at most 4 bytes of context. The high-order context model (orders 5–8) partially addresses this, but LZMA’s sliding window (up to 64 MB) captures much longer repetitions.
3. **Binary data.** MIDICOTH is optimized for text. On binary data (executables, images), the word model and high-order context model provide little benefit, and compression ratios are worse than specialized binary compressors.
4. **Single-threaded.** The current implementation processes bytes sequentially on a single core. The pipeline’s adaptive, sequential nature makes parallelization non-trivial.

6.6 Future Work

1. **Higher PPM orders.** Extending to order-6 or order-8 directly within PPM (with appropriate memory management) could close the gap to dictionary methods on small files.
2. **More denoising steps.** Currently $K = 3$ steps are used. Investigating whether additional steps with finer calibration granularity yield diminishing or continued returns.
3. **Specialized binary models.** Adding models for structured binary formats (e.g., x86 instruction decoding, image pixel prediction) would improve performance on non-text data.
4. **Theoretical analysis of optimal calibration granularity.** The current calibration table dimensions (27 bit contexts, 4 shape bins, 8 confidence bins, 20 probability bins) were determined empirically. An information-theoretic analysis relating optimal bin counts to input size and prior strength could guide further improvements.

7. Conclusion

We have presented MIDICOTH, a lossless compression system built around *micro-diffusion*—a multi-step score-based reverse diffusion process that treats PPM predictions as noisy observations corrupted by the Jeffreys prior and applies Tweedie’s empirical Bayes formula to denoise them. The additive correction $\hat{\delta} = \hat{E}[\theta|\hat{p}] - \hat{E}[\hat{p}]$, a consistent estimate of the optimal additive correction (approximating the Tweedie term $\sigma^2 \cdot s(\hat{p})$), is computed nonparametrically via calibration tables conditioned on the noise level.

Our primary contributions are:

First, the binary tree Tweedie denoiser, applied as the final post-blend correction step, provides a consistent 2.3–2.7% reduction in compressed size across all tested datasets. Critically, placing Tweedie *after* all model blending (match, word, high-order context) allows it to calibrate the entire ensemble’s output, not just the PPM base model. The technique is general: it can be applied as a post-processing step to any ensemble of context models that provides a probability distribution and a confidence estimate, without modifying the underlying models.

Second, the binary tree decomposition and enriched bit contexts enable data-efficient calibration that scales gracefully from small files (152 KB) to large ones (100 MB). The 27 bit contexts, encoding tree level and parent path, allow the calibration to distinguish qualitatively different byte ranges without requiring prohibitive amounts of data.

Third, the full five-layer pipeline achieves 1.753 bpb on enwik8 (100 MB), outperforming xz -9 (1.989 bpb) by 11.9%, and 2.119 bpb on alice29.txt, outperforming xz -9 (2.551 bpb) by 16.9%—using only adaptive statistical models with no neural network, no training data, no GPU. This demonstrates that significant compression improvements remain achievable through algorithmic innovation in classical statistical modeling.

The entire system is implemented in $\sim 2,000$ lines of C with no external dependencies, compresses at ~ 60 KB/s on a single CPU core, and is fully deterministic with bit-exact encoder–decoder symmetry.

Code availability. MIDICOTH is open-source and available at <https://github.com/robtacconelli/midicoth>.

References

- [1] Arnold, R. and Bell, T. (1997). A corpus for the evaluation of lossless compression algorithms. In *Data Compression Conf. (DCC '97)*, pp. 201–210.
- [2] Bellard, F. (2023). ts_zip: Text compression using large language models. https://bellard.org/ts_zip/.
- [3] Cleary, J. G. and Witten, I. H. (1984). Data compression using adaptive coding and partial string matching. *IEEE Transactions on Communications*, 32(4):396–402.
- [4] Efron, B. (2012). *Large-Scale Inference: Empirical Bayes Methods for Estimation, Testing, and Prediction*. Cambridge University Press.
- [5] Delétang, G., Ruoss, A., Duquenne, P.-A., et al. (2024). Language modeling is compression. In *Proceedings of ICLR 2024*. arXiv:2309.10668.
- [6] Efron, B. (2011). Tweedie’s formula and selection bias. *Journal of the American Statistical Association*, 106(496):1602–1614. doi:10.1198/jasa.2011.tm11181.
- [7] Fowler, G., Noll, L. C., and Vo, P. (1991). FNV hash. <http://www.isthe.com/chongo/tech/comp/fnv/>.
- [8] Guo, C., Pleiss, G., Sun, Y., and Weinberger, K. Q. (2017). On calibration of modern neural networks. In *Proceedings of ICML 2017*.
- [9] Ho, J., Jain, A., and Abbeel, P. (2020). Denoising diffusion probabilistic models. In *Advances in NeurIPS 2020*.
- [10] James, W. and Stein, C. (1961). Estimation with quadratic loss. In *Proc. 4th Berkeley Symposium on Mathematical Statistics and Probability*, vol. 1, pp. 361–379.
- [11] Huffman, D. A. (1952). A method for the construction of minimum-redundancy codes. *Proceedings of the IRE*, 40(9):1098–1101.
- [12] Mittu, F., Bu, Y., et al. (2024). FineZip: Pushing the limits of large language models for practical lossless text compression. *arXiv preprint*, arXiv:2409.17141.
- [13] Jeffreys, H. (1946). An invariant form for the prior probability in estimation problems. *Proceedings of the Royal Society A*, 186(1007):453–461.
- [14] Knoll, B. (2024). CMIX: A lossless data compression program. <http://www.byronknoll.com/cmix.html>.
- [15] Knoll, B. and de Freitas, N. (2011). A machine learning perspective on predictive coding with PAQ. *arXiv preprint*, arXiv:1108.3298.
- [16] Moffat, A. (1990). Implementing the PPM data compression scheme. *IEEE Transactions on Communications*, 38(11):1917–1921.
- [17] Mahoney, M. (2005). Adaptive weighing of context models for lossless data compression. Technical Report, Florida Institute of Technology.
- [18] Mahoney, M. (2023). Large text compression benchmark. Available at: <http://mattmahoney.net/dc/text.html>. Accessed March 2026.
- [19] Shannon, C. E. (1948). A mathematical theory of communication. *Bell System Technical Journal*, 27(3):379–423.
- [20] Song, Y., Sohl-Dickstein, J., Kingma, D. P., et al. (2021). Score-based generative modeling through stochastic differential equations. In *Proceedings of ICLR 2021*. arXiv:2011.13456.
- [21] Tacconelli, R. (2025). Nacriith: Neural lossless compression via ensemble context modeling and high-precision CDF coding. *arXiv preprint*, arXiv:2602.19626.
- [22] Witten, I. H., Neal, R. M., and Cleary, J. G. (1987). Arithmetic coding for data compression. *Communications of the ACM*, 30(6):520–540.

- [23] Ziv, J. and Lempel, A. (1977). A universal algorithm for sequential data compression. *IEEE Transactions on Information Theory*, 23(3):337–343.